

# Crystal and Magnetic Structure of PrCaCrO<sub>4</sub>

J. Romero de Paz,\* M. T. Fernández-Díaz,† J. Hernández Velasco,‡ R. Sáez Puche,‡<sup>1</sup> and J. L. Martínez§

\*Departamento de Química Inorgánica y Materiales, Facultad de Ciencias Experimentales y Técnicas, Universidad San Pablo CEU, E-28660 Boadilla del Monte, Madrid, Spain; †Institut Laue-Langevin, BP 156X, F-38042 Grenoble Cedex, France; ‡Departamento de Química Inorgánica, Facultad de Ciencias Químicas, Universidad Complutense, E-28040 Madrid, Spain; and §Instituto de Ciencia de Materiales del CSIC, Cantoblanco E-28049 Madrid, Spain

Received January 27, 1998; in revised form July 22, 1998; accepted July 23, 1998

The crystal and magnetic structures of PrCaCrO<sub>4</sub> have been characterized by high-resolution neutron diffraction. The structure is described as orthorhombic with space group *Bmab* and lattice parameters  $a = 5.3909(3)$  Å,  $b = 5.3999(3)$  Å, and  $c = 11.9932(5)$  Å at 200 K. The antiferromagnetic ordering in the Cr<sup>3+</sup> sublattice is explained on the basis of a propagation vector  $k = 0$  and a collinear structure, described within a symmetry mode  $G_x$  and a magnetic moment of  $2.38(9)$  μ<sub>B</sub> at 1.5 K. The Néel temperature is around 180 K from both neutron diffraction and magnetic susceptibility measurements. © 1999 Academic Press

**Key Words:** Antiferromagnetism; neutron powder diffraction; magnetic structure.

## 1. INTRODUCTION

RCaCrO<sub>4</sub>, where *R* = rare earth element, form a family of compounds which crystallize with a distorted K<sub>2</sub>NiF<sub>4</sub> structural type. The structure can be described as formed by CrO<sub>2</sub> planes separated by RCaO<sub>2</sub> bilayers along the *c*-axis. The R<sup>3+</sup> and Ca<sup>2+</sup> cations are randomly distributed in the 8*f* sites of the space group *Bmab*, in which these oxides crystallize (1).

When R<sup>3+</sup> is a diamagnetic cation, for example, La<sup>3+</sup> or Y<sup>3+</sup>, the interlayer magnetic interactions between the CrO<sub>2</sub> planes will be diminished and the corresponding compounds will show a two-dimensional behavior. Concerning the evolution from two- to three-dimensional magnetic behavior, many studies have been reported in the case of the oxides A<sub>2-x</sub>R<sub>x</sub>MO<sub>4</sub>, where *A* is an alkaline earth, such as Sr<sup>2+</sup> or Ca<sup>2+</sup>, and *M* = Mn and Fe. It has been reported that both the structure and the magnetic properties are strongly dependent on the amount of doping *x* (2–7). However, only a few studies have been reported in the case of the RCaCrO<sub>4</sub> (1, 8, 9). The decreasing size of rare earth ion from Nd to Y increases the so-called orthorhombic strain because

of the tilt of CrO<sub>6</sub> octahedra in the perovskite layers of this structure (1). In the case of YCaCrO<sub>4</sub>, a high-temperature phase transition at about 1400°C has also been reported (9), but the study of the magnetic properties reveals the onset of a ferromagnetic signal assigned to YCrO<sub>3</sub> impurity, which behaves as an antiferromagnet with a ferromagnetic canting at 141 K, which is the Néel temperature (10). Moreover, the different RCaCrO<sub>4</sub> obtained from the stoichiometric amounts of reactants, using the ceramic method, always show different amounts of impurities of the perovskites RCrO<sub>3</sub>, which make difficult the study of the magnetic properties (11, 12).

The aims of this work are the synthesis of PrCaCrO<sub>4</sub> as a pure phase, its characterization by high-resolution neutron diffraction, and the study of its magnetic properties from magnetic susceptibility and neutron diffraction data obtained at different temperatures.

## 2. EXPERIMENTAL

PrCaCrO<sub>4</sub> was prepared as a pure sample from the stoichiometric amounts of high-purity Pr<sub>6</sub>O<sub>11</sub> (99.99%), Cr<sub>2</sub>O<sub>3</sub> (99.9%), and a large excess of CaCO<sub>3</sub> to avoid the presence of PrCrO<sub>3</sub> and to accelerate the reaction rate. This mixture was ground and heated under argon flow at 1380°C for 64 h and one interruption was made for grinding the sample.

Neutron powder diffraction experiments were carried out using the High Flux Reactor facilities of the Institut Laue-Langevin (Grenoble, France). The data were collected using the high-resolution powder diffractometer D2B ( $\lambda = 1.5945$  Å) at different temperatures from 300 to 1.5 K over an angular range of  $1.0^\circ < 2\theta < 161.95^\circ$  with steps of  $0.05^\circ$ . All the data were analyzed with the Rietveld method using the program Fullprof (13). A pseudo-Voigt profile function was used for describing the peak shape.

Magnetic susceptibility data were recorded using a Quantum Design MPMS SQUID magnetometer in the 1.7–300 K

<sup>1</sup>To whom correspondence should be addressed.

temperature range. The magnetic field was 500 Oe and the samples were zero field cooled (ZFC) prior to the magnetic measurements. The setup was calibrated with metallic Pd as standard and the data were corrected for ionic diamagnetism.

### 3. RESULTS AND DISCUSSION

#### 3.1. Structural Features

Figure 1a shows the high-resolution neutron diffraction pattern obtained at 200 K for PrCaCrO<sub>4</sub>. The data have been refined assuming the symmetry of space group *Bmab*, and traces of CaO (<4%) have been taken into account. The main structural data are displayed in Table 1. Although the Cr<sup>3+</sup> electronic configuration is isotropic (3d<sup>3</sup>), the CrO<sub>6</sub> octahedra are axially elongated with a ratio  $d(\text{Cr-O})_{\text{ax}}/d(\text{Cr-O})_{\text{eq}} = 1.07$ . The orthorhombic distortion is a consequence of the tilting of the octahedra in the **ab** plane. The tilt angles take the values of  $\alpha_1 = 4.0(3)^\circ$  (the angle between the axial octahedral bond and the **c**-axis) and  $\alpha_2 = 4.9(2)^\circ$  (the angle formed by the equatorial octahedral plane with the crystal **ab** plane). The orthorhombic distortion is rather small and appears to increase gradually when the praseodymium is replaced by smaller lanthanide elements.

It is worth noting that the symmetry and the space group *Bmab* remain unchanged down to 1.5 K. This result is rather surprising if it is compared with the isostructural *R*<sub>2</sub>MO<sub>4</sub> (*M* = Ni and Cu), for which temperature-induced phase transitions of the type orthorhombic to tetragonal symmetry have been reported when the temperature is lowered (14–16).

**TABLE 1**  
Lattice Parameters, Atomic Coordinates, and Conventional Discrepancy Factors from Rietveld Refinement of Neutron Diffraction Data Obtained at 200 and 1.5 K<sup>a</sup>

Atom	Site	<i>x</i>	<i>y</i>	<i>z</i>
200 K: <i>a</i> = 5.3909(3) Å <i>b</i> = 5.3999(3) Å <i>c</i> = 11.9932(5) Å				
1.5 K: <i>a</i> = 5.3877(3) Å <i>b</i> = 5.3928(3) Å <i>c</i> = 11.9818(4) Å				
Pr/Ca	8 <i>f</i>	0	−0.0083(10) −0.0092(10)*	0.3588(4) 0.3586(4)*
Cr	4 <i>a</i>	0	0	0
O1	8 <i>e</i>	0.25	0.25	−0.0079(5) −0.0083(4)*
O2	8 <i>f</i>	0	0.0324(10) 0.0345(8)*	0.1689(4) 0.1691(3)*
200 K: <i>R</i> <sub>p</sub> = 20.4% <i>R</i> <sub>wp</sub> = 17.9% <i>R</i> <sub>exp</sub> = 11.27% $\chi^2 = 2.52$ <i>R</i> <sub>B</sub> = 6.59%				
1.5 K: <i>R</i> <sub>p</sub> = 15.3% <i>R</i> <sub>wp</sub> = 14.3% <i>R</i> <sub>exp</sub> = 7.21% $\chi^2 = 3.92$ <i>R</i> <sub>B</sub> = 5.45%				

<sup>a</sup>Data at 1.5 K are indicated with an asterisk.

#### 3.2. Magnetic Behavior

Figure 2 shows the temperature dependence of the magnetic susceptibility. It can be observed that the susceptibility obeys a Curie–Weiss law,  $\chi = 2.73/(T - 181.4)$ , between 300 and 200 K. The magnetic moment calculated for this temperature range is 4.67(1)  $\mu_B$ , which is slightly lower than that expected for Pr<sup>3+</sup> and Cr<sup>3+</sup> paramagnetic contribution, i.e., 5.27  $\mu_B$ . This reduction in the effective magnetic moment could be due to 2D correlations in the layered chromium sublattice, which are characteristic of this structure. The purity of this sample is confirmed by the nonexistence of any anomaly at 238.7 K, which is the *T*<sub>N</sub> of PrCrO<sub>3</sub> (17).

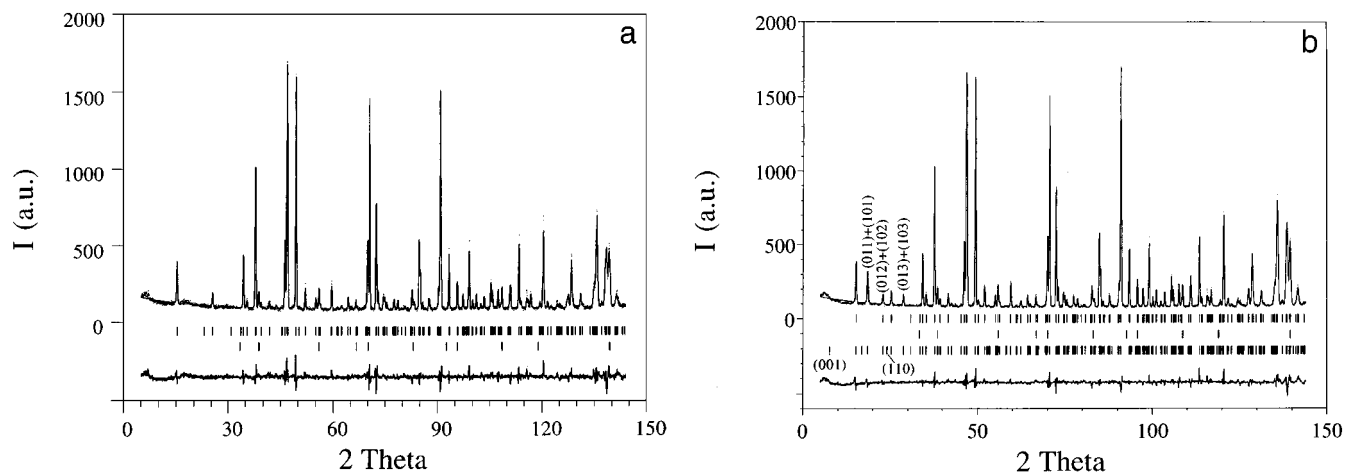


**FIG. 1.** (a) Neutron powder diffraction pattern obtained at 200 K for PrCaCrO<sub>4</sub>. (b) Neutron powder diffraction pattern obtained at 1.5 K. Experimental, calculated, and difference diagrams are plotted. Vertical marks show the allowed structural and magnetic Bragg reflections for PrCaCrO<sub>4</sub> (first and third rows, respectively) and CaO (second row).

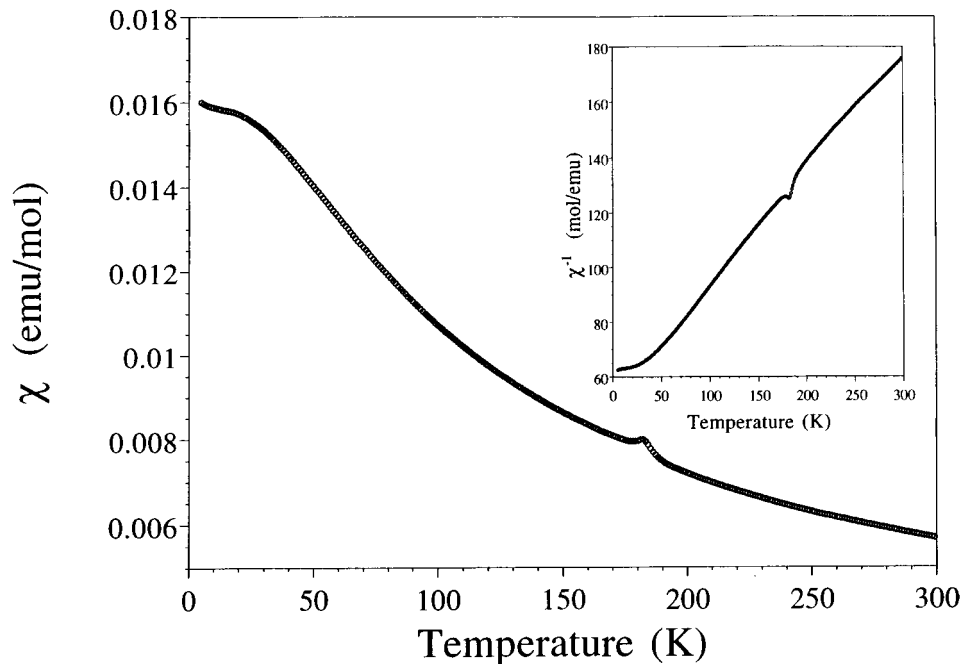


FIG. 2. Magnetic susceptibility thermal dependence for PrCaCrO<sub>4</sub>. Reciprocal susceptibility is shown in the inset.

Around 180 K, one can observe a marked anomaly, which is due to the 3D antiferromagnetic ordering in the Cr<sup>3+</sup> sublattice. Below this temperature, the calculated magnetic moment, 4.20(1)  $\mu_B$ , corresponds to the value of Pr<sup>3+</sup> and some contribution from the remaining paramagnetic signal of the Cr<sup>3+</sup>. Below 40 K, temperature-independent paramagnetism is observed, which is the characteristic behavior of the <sup>3</sup>H<sub>4</sub> ground term of Pr<sup>3+</sup>.

Neutron diffraction study at different temperatures fully confirms the 3D antiferromagnetic ordering in the chromium sublattice below 200 K. The magnetic reflections have been indexed on the basis of a propagation vector  $\mathbf{k} = [0, 0, 0]$ . The neutron diffraction pattern at 1.5 K is shown in Fig. 1b.

The basis vector components for the irreducible representations which could describe the magnetic order for the Cr sublattices were obtained by using representation analysis and taking as generators of *Bmab* space group the following symmetry operations: the *B*-centering translation  $t(\frac{1}{2}, 0, \frac{1}{2})$ , the helical axis 2<sub>1y</sub>, and the rotation axis 2<sub>z</sub>. Bertaut's notation is used for the linear spin combinations (18); see Table 2. By contrast with the isostructural R<sub>2</sub>NiO<sub>4</sub> (19), in which the rare earth ions are also involved in the magnetic ordering, in the case of PrCaCrO<sub>4</sub> it is worth noting that the Pr<sup>3+</sup> remains disordered down to 1.5 K. This behavior was expected because of the random distribution of Ca<sup>2+</sup> and Pr<sup>3+</sup> in the 8*f* sites. See Table 1.

From the evaluation of the magnetic structure factor, it is possible to infer some general considerations limiting the

existence of magnetic reflections affecting the parity of the Miller indices that are shown in Table 2. It is worth noting that the highest intensity magnetic peaks correspond to reflections (011) or (101) and (013) or (103), shown in Fig. 1b, which are allowed only for the *G* or *C* modes, respectively. Moreover, there is an indication of a coupling of spins mainly directed along the *x* or *y* direction. The nonexistence

TABLE 2  
Basis Vectors for the Irreducible Representations of Cr Sublattices in *Bmab* ( $\mathbf{k} = 0$ ) and Rules for Allowed Magnetic Reflections<sup>a</sup>

	<i>x</i>	<i>y</i>	<i>z</i>
Γ <sub>1</sub> (+++)	<i>C</i>	—	—
Γ <sub>2</sub> (++-)	—	<i>F</i>	<i>C</i>
Γ <sub>3</sub> (+-+)	—	<i>C</i>	<i>F</i>
Γ <sub>4</sub> (-++)	—	<i>G</i>	<i>A</i>
Γ <sub>5</sub> (+--)	<i>F</i>	—	—
Γ <sub>6</sub> (-+-)	<i>A</i>	—	—
Γ <sub>7</sub> (--+)	<i>G</i>	—	—
Γ <sub>8</sub> (---)	—	<i>A</i>	<i>G</i>

$$F = S_1 + S_2 + S_3 + S_4; h + l = 2n, k + l = 2n, h + k = 2n$$

$$G = S_1 - S_2 + S_3 - S_4; h + l = 2n + 1, k + l = 2n, h + k = 2n + 1$$

$$C = S_1 + S_2 - S_3 - S_4; h + l = 2n, k + l = 2n + 1, h + k = 2n + 1$$

$$A = S_1 - S_2 - S_3 + S_4; h + l = 2n + 1, k + l = 2n + 1, h + k = 2n$$

<sup>a</sup> S<sub>*i*</sub> represents a spin component of atom in *i* sublattice of the 4*a* site and *n* is an arbitrary integer.

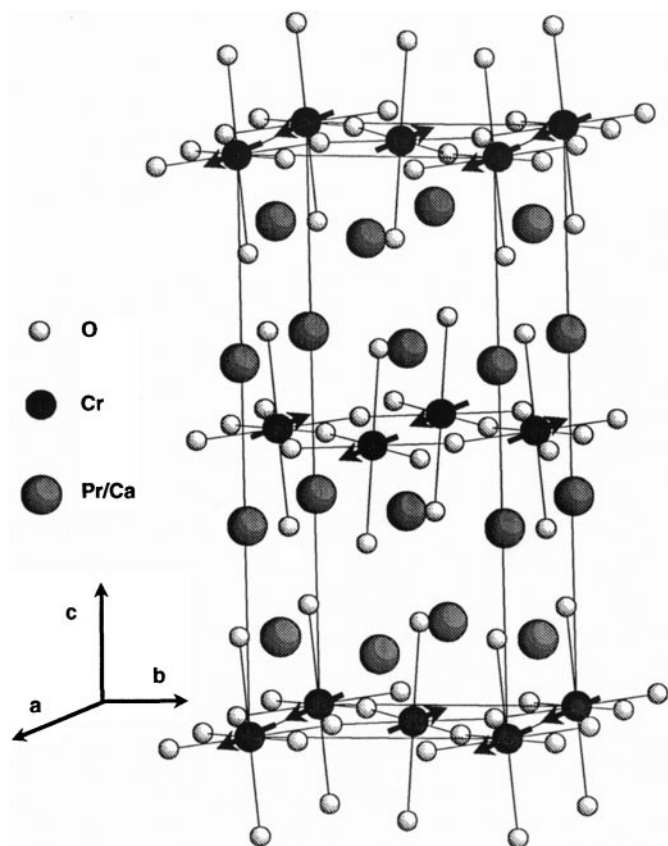


FIG 3. Representation of the magnetic structure of  $\text{PrCaCrO}_4$  in the crystal unit cell.

of reflections (001) and (110) and no magnetic scattering contribution to the intensity at the nuclear peak positions permit us to leave out the  $A$  and  $F$  modes, respectively. The fitting of experimental data agrees with either a  $G_x$  or a  $C_y$  mode, in the latter case the coupling within the  $\Gamma_3$  (+ - +) representation with  $F_z = 0$ . Due to the pseudotetragonal symmetry of the crystal structure, it is rather difficult to distinguish between these modes. The discrepancy factors for the fitting of both models are almost the same ( $R_M = 13\%$ ). We labeled the four Cr magnetic sublattices in Wyckoff site  $4a$ : 1 (0, 0, 0), 2 ( $\frac{1}{2}, 0, \frac{1}{2}$ ), 3 ( $0, \frac{1}{2}, \frac{1}{2}$ ), and 4 ( $\frac{1}{2}, \frac{1}{2}, 0$ ). Figure 3 shows the magnetic structure with a  $G_x$  spin configuration; it can be observed that turning  $90^\circ$  around the

$c$ -direction yields a  $C_y$  arrangement for equal  $a$  and  $b$  parameters. The obtained value for the  $\text{Cr}^{3+}$  magnetic moment is  $2.38(9) \mu_B$  at 1.5 K and it is oriented along either the  $x$  or the  $y$  direction respectively for the proposed models, but doubtless perpendicular to the crystallographic  $c$ -axis.

#### ACKNOWLEDGMENTS

The authors thank the Comisión Interministerial de Ciencia y Tecnología for financial support under Project MAT96-0975.

#### REFERENCES

1. A. Daoudi and G. Le Flem, *Mater. Res. Bull.* **8**, 1103 (1973).
2. A. Daoudi and G. Le Flem, *J. Solid State Chem.* **5**, 57 (1972).
3. C. Chaumont, A. Daoudi, G. Le Flem, and P. Hagenmuller, *J. Solid State Chem.* **14**, 335 (1975).
4. J. C. Bouloux, J. L. Soubeyrou, A. Daoudi, and G. Le Flem, *Mater. Res. Bull.* **16**, 855 (1981).
5. J. Takahashi and N. Kamegashira, *Mater. Res. Bull.* **28**, 451 (1993).
6. J. L. Soubeyrou, P. Courbin, L. Fournes, D. Fruchart, and G. Le Flem, *J. Solid State Chem.* **31**, 313 (1980).
7. M. M. Nguyen-Trut-Dinh, M. Vlasse, M. Perrin, and G. Le Flem, *J. Solid State Chem.* **32**, 1 (1980).
8. Ch. Chaumont, G. Le Flem, P. Hagenmuller, *Z. Anorg. Allg. Chem.* **470**, 18 (1980).
9. R. Berjoan, J. P. Coutures, G. Le Flem, and M. Saux, *J. Solid State Chem.* **42**, 75 (1982).
10. J. B. Goodenough and J. M. Longo, in "Crystallographic and Magnetic Properties of Perovskites and Perovskite-Related Compounds," Landolt-Bornstein Vol. 4. Springer-Verlag, Berlin, 1970.
11. J. Romero, R. Sáez Puche, F. Fernández, J. L. Martínez, Q. Chen, R. Burriel, and M. Castro, *J. Alloys Compd.* **225**, 203 (1995).
12. J. L. Martínez, M. T. Fernández-Díaz, Q. Chen, C. Prieto, A. de Andrés, R. Sáez Puche, and J. Romero, *J. Magn. Magn. Mater.* **140-144**, 1179 (1995).
13. J. Rodríguez-Carvajal, in "Abstracts of Satellite Meeting on Powder Diffraction of the XV Congress of the International Union of Crystallography," Toulouse, 1990, p. 127.
14. J. Rodríguez-Carvajal, J. L. Martínez, J. Pannetier, and R. Sáez-Puche, *Phys. Rev. B* **38**, 7148 (1988).
15. M. T. Fernández Díaz, Ph.D. Thesis, Universidad Autónoma de Madrid, Madrid, 1991.
16. J. Lander, P. J. Brown, J. Spalek, and J. M. Honig, *Phys. Rev. B* **40**, 4463 (1989).
17. S. Quezel-Ambrunaz and M. Mareschal, *Bull. Soc. Fr. Miner. Cryst.* **86**, 204 (1963).
18. E. F. Bertaut, in "Magnetism" (G. T. Rado and H. Suhl, Eds.), Vol. III, p. 149. Academic Press, New York, 1963.
19. J. Rodríguez-Carvajal, M. T. Fernández-Díaz, J. L. Martínez, F. Fernández, and R. Saéz-Puche, *Europhys. Lett.* **11**, 261 (1990).